Integrating Environmental Variables and Machine Learning for Wildfire Susceptibility Prediction in Portugal

Authors

- Mohamed Amine Laghmich[1] (https://orcid.org/0009-0008-4503-4358)
- Mohammed Ariche[1] (https://orcid.org/0009-0009-8259-0537)
- Bouthaina Ahayk[1] (https://orcid.org/0009-0001-3385-1069)

Affiliation

[1] Faculty of Humanities and Social Sciences, Department of Geography, Ibn Tofail University, Kenitra, Morocco

Corresponding author:
Mohamed Amine Laghmich
Email: mohamedamine.laghmich@uit.ac.ma

Preprint Status Statement

This manuscript is a non-peer-reviewed preprint submitted to EarthArXiv.

Abstract: Wildfires constitute a significant ecological disturbance within Mediterranean ecosystems, exerting profound effects on forest dynamics, biodiversity, and land management practices. The development of precise susceptibility mapping is essential to inform prevention strategies, optimize resource allocation, and promote sustainable forest management by increasing fire pressure. This study employed and compared four machine learning classifiers—Random Forest, Classification and Regression Trees (CART), Gradient Boosting, and Extreme Gradient Boosting (XGBoost)—to model wildfire susceptibility across Portugal. Six environmental and anthropogenic predictors were utilized: vegetation indices, land use/land cover, slope, elevation, wind speed, and distance to settlements. The results indicated that vegetation-related variables, particularly NDVI and land cover, were the most significant determinants of fire occurrence, followed by slope and wind speed, thus underscoring the role of biophysical conditions in shaping fire regimes. Among the evaluated models, XGBoost demonstrated the highest predictive performance (overall accuracy = 92.98%, AUC = 0.98), surpassing or equalling the other ensemble methods. The resulting susceptibility maps identified the northern and central interior regions as the most fire-prone, consistent with historical fire records. Our findings underscore the efficacy of ensemble machine learning techniques in capturing complex fire–environment interactions and provide spatially explicit information that can enhance fire prevention planning, support conservation priorities, and guide adaptive forest management in Mediterranean landscapes.

Keywords
Wildfire susceptibility; Machine learning; Ensemble classifiers; Forest fire risk assessment; Remote sensing and GIS; Mediterranean ecosystems; Forest management

1. Introduction

Portugal, distinguished by its Mediterranean climate and dynamic land use and land cover (LULC) changes, has witnessed evolving wildfire trends that present significant environmental and socio-economic challenges (Oliveira & Zêzere, 2020; Parente et al., 2018). The Mediterranean region is particularly susceptible to wildfires because of its hot, dry summers, frequent droughts, and vegetation that is prone to ignition. In recent years, extreme heatwaves with temperatures surpassing 48°C have precipitated devastating wildfires across Mediterranean countries, resulting in loss of life, extensive property damage and environmental degradation (Turco et al., 2017). For instance, in Portugal, over 3,370 rural fires consumed 25,4295 hectares of land in Jan to Aug of 2025, which was to more three times the area burned during the same period in 2024 (ICNF, 2025).

The accumulation of dry vegetation and human activities in proximity to forested areas heightens the risk of uncontrollable mega-fires that often exceed firefighting capacities. In Portugal, climate change coupled with trends in rural land abandonment and land use changes has led to increased fuel loads and wildfire incidents (Eurostat, 2025; Sabater et al., 2021). These fires pose threats to lives, ecosystems, and economic assets and significantly contribute to carbon emissions. For instance, wildfires across the European Union in 2025, up to late August, released an estimated 38.37 million tonnes of CO2, reaching a record high for that time period (European Commission, 2025).

Despite the recognized dangers, wildfire management in the Mediterranean region typically emphasizes full suppression, which can paradoxically elevate the risk of larger and more intense fires by permitting fuel accumulation (Fernandes & Botelho, 2003). Despite advancements in wildfire susceptibility modelling, critical gaps related to spatial bias and overly optimistic model validation persist, potentially limiting their accuracy and practical applicability (Jaafari & Pourghasemi, 2019; Parente et al., 2018). Addressing these issues is crucial for enhancing the reliability of fire-risk predictions and supporting effective wildfire prevention and mitigation strategies.

This study addresses these gaps by pursuing two primary objectives: first, to systematically compare the performance of four ensemble machine learning models—Random Forest, CART, Gradient Boosting, and XGBoost—for wildfire susceptibility mapping in Portugal; and second, to identify and evaluate the most influential environmental and anthropogenic predictors driving fire occurrence in the region. The findings provide a robust framework for wildfire risk assessment, offering spatially explicit insights to inform management and policy

decisions. By integrating the understanding of wildfire dangers specific to Mediterranean environments and addressing modelling limitations, this study aims to contribute to more accurate, reliable, and spatially explicit wildfire risk assessments in Portugal. This will aid in adopting proactive fire management strategies that balance suppression and ecosystem resilience, thereby helping to mitigate the impacts of wildfires in a changing climate.

2. Materials and Methods

2.1 Study Area

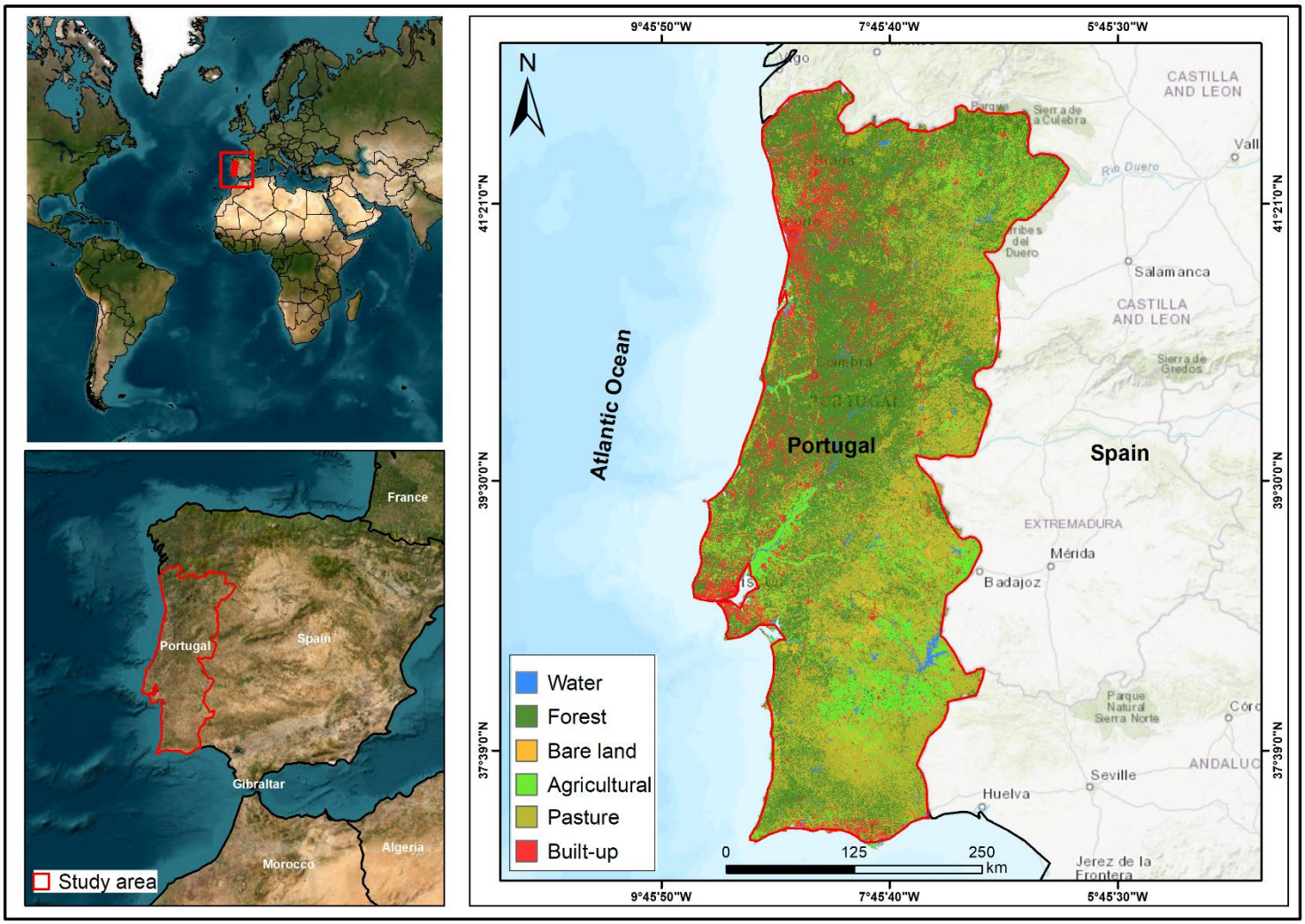

Figure 1. Study area location.

Portugal, situated at approximately 39.4° N, 8.22° W on the Iberian Peninsula, has a total area of 92,212 km² and a population of approximately 10.2 million (Central Intelligence Agency 2025). The country has a Mediterranean climate with hot, dry summers and mild, wet winters

(Oliveira & Zêzere, 2020; Parente et al., 2018). Combined with the varied topography and extensive forest cover, this climate makes Portugal highly susceptible to wildfires during the summer months.

The landscape is a mosaic of forests, shrublands, agricultural land and settlements. Forests cover approximately 36% of the territory (Eurostat, 2025), with fire-prone regions concentrated in the northern and central inland districts, such as Vila Real, Braga, Aveiro and Coimbra. Mountainous terrain with steep slopes and dense vegetation further increases wildfire risk due to fuel accumulation and enhanced fire spread potential (Sabater et al., 2021).

Wildfires have intensified in recent years. In the first seven months of 2025, over **7,32 rural fires** were recorded, burning approximately **254,295 hectares** across the country (Figure 2.) (ICNF, 2025). These events affected regions nationwide, causing widespread damage and evacuations.
Land use and land cover (LULC) changes also play critical roles. Rural depopulation and land abandonment contribute to higher fuel loads, whereas flammable eucalyptus and maritime pine plantations exacerbate fire intensity under drought conditions, which are aggravated by climate change.

This combination of environmental, climatic, and human pressures makes Portugal a challenging study area for wildfire prediction. Understanding the spatial and temporal fire susceptibility patterns of this species is essential for advancing prevention strategies and risk mitigation.

2.2 Historical Forest Fires

The historical forest fire data for this study were sourced from the **Institute for Nature Conservation and Forests (ICNF)** of Portugal, the principal national authority responsible for forest and wildfire monitoring. The ICNF database contains detailed records of fire incidents, including annual fire counts and total burned areas, and offers a comprehensive overview of wildfire trends in Portugal from 2006 to 2025 (ICNF, 2025).
As illustrated in **Figure 2**, from 2006 to 2013, the annual fire counts exceeded 25,000 events, peaking at nearly 30,000 fires around 2013. Since 2020, fewer than 10, 000 fires have been reported annually, indicating a significant decline in fire frequency.

The patterns of burned areas exhibited greater interannual variability (Figure 2).
Most years between 2006 and 2024 experienced burned areas ranging from 50,000 to 200,000 hectares. However, 2017 was notable as an extreme fire season, with over 500,000 hectares burned (Turco et al., 2019). Following this peak, the annual burned areas generally remained lower, although recent increases in 2024–2025 suggest a potential resurgence of large-scale fire activity. In 2025 (January to August), the burned area exceeded 254,000 hectares.
These data reflect the evolving fire regime in Portugal and underscore the importance of the long-term monitoring capabilities maintained by ICNF. Detailed ICNF records serve as both a historical context and a crucial validation reference for this study's analysis and modelling of wildfire susceptibility (Almeida et al., 2024).

Overall, the historical analysis demonstrates that while the number of fires has decreased over time, the magnitude of burned areas remains highly variable, reflecting the strong influence of climatic extremes, vegetation conditions, and human factors. These findings highlight the need for robust susceptibility modelling and spatial planning to mitigate the risk of severe fire events in the region.

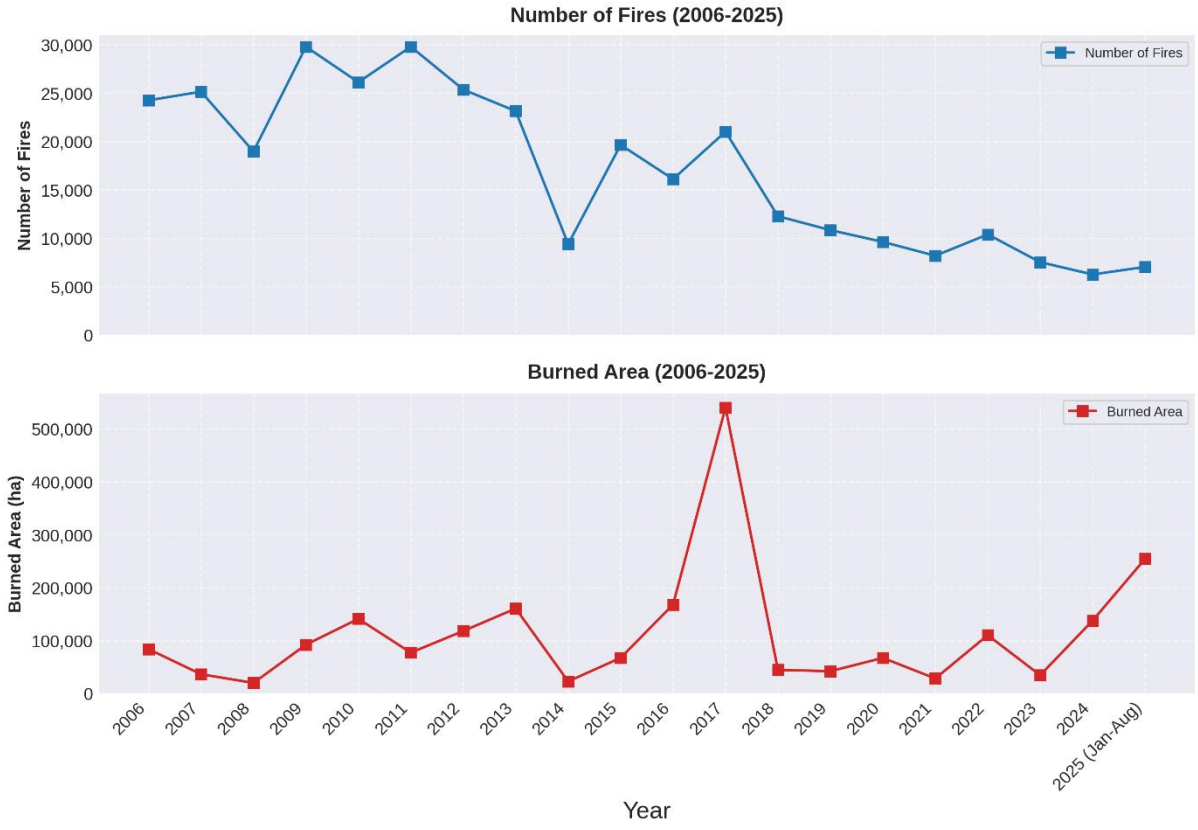

Figure 2. Number of forest fires (top) and burned area in hectares (bottom) in Portugal from 2006 to August 2025 based on the ICNF historical wildfire records.

2.3 Data Collection and Sample Generation

The wildfire susceptibility modelling in this study was based on a binary dependent variable: fire presence or absence. Fire presence data were obtained from the MODIS Active Fire product (MCD14ML, FIRMS) for the period 2015–2024 (Giglio et al., 2016).

The dataset was subjected to a cleaning process to ensure its ecological relevance and accuracy.

Specifically, fire detections located within built-up areas were removed to restrict the analysis to forest and shrubland fires, and spurious detections, such as single isolated pixels and cloud-related anomalies, were also excluded.

From this cleaned dataset, 1,000 fire points were randomly selected as the positive samples.

To create a balanced dataset, an equal number of no-fire points (1,000) were randomly generated in areas that showed no active fire detection during the same period (Tonini et al., 2020).

A minimum buffer distance was applied to ensure no spatial overlap with the fire pixels. A final balanced dataset of 2,000 samples was used for model training and validation.

2.4 Explanatory Variables

The six explanatory variables were downloaded and processed using Google Earth Engine (GEE), which provides convenient access to extensive satellite imagery and geospatial datasets with planetary-scale computational capabilities. The use of GEE allowed for the efficient extraction of variable values at 2,000 sample points directly at their native spatial resolutions, facilitating consistent and reproducible data preparation for model training without the need for potentially bias-inducing resampling procedures.

- **Vegetation:** NDVI (2015–2024 average) derived from Landsat 8 and 9 surface reflectance images (Vermote et al., 2016).
- **Topography:** Slope derived from the 30 m SRTM DEM (Farr et al., 2007).
- **Human Pressure:** Distance to settlements calculated from the GHSL Built-Up product (2024) using a Euclidean distance transform (European Commission. Joint Research Centre., 2024; Verde & Zêzere, 2010).
- **Land Cover:** LULC extracted from the Dynamic World product (Sentinel-2, 10 m) for 2024 (Brown et al., 2022).

- **Climate:** Land surface temperature (LST) from MODIS Terra (MOD11A2.061) and Aqua (MYD11A2.061), averaged for 2015–2024 (1 km) (Wan et al., 2021).
- **Climate:** Wind speed from ERA5-Land reanalysis, averaged for 2015–2024 (1 km) (Muñoz-Sabater et al., 2021).

Table 1. Summary of variables used in wildfire susceptibility modelling

Variable	Description	Source	Spatial Resolution	Temporal Coverage	Units
Fire presence	Active fire detections	MODIS Active Fire Product (MCD14ML, FIRMS)	~1 km	2015–2024	Binary (presence/absence)
NDVI	Proxy for vegetation greenness and fuel availability	Landsat 8 & 9 SR (USGS/NASA)	30 m	2015–2024 (average)	Index (−1 to +1)
Slope	Topographic steepness derived from DEM	SRTM DEM (NASA/USGS)	30 m	Static	Degrees (°)
Distance to settlements	Euclidean distance from built-up areas	GHSL Built-Up (EC–JRC, 2024)	100 m	2024	Meters (m)
Land Cover (LULC)	Land cover classes (forest, cropland, shrubland, etc.)	Dynamic World (Sentinel-2)	10 m	2024	Categorical
LST	Land Surface Temperature	MODIS Terra (MOD11A2.061) & Aqua (MYD11A2.061)	1 km	2015–2024 (average)	°C
Wind speed	Surface wind speed	ERA5-Land reanalysis (ECMWF)	10 km	2015–2024 (average)	m/s

2.5 Methodology workflow

The methodology of this study followed a structured workflow for predicting wildfire susceptibility, as illustrated in **Figure 3**. The process began with data preparation and continued with machine learning model development, validation, and the final generation of the susceptibility maps.

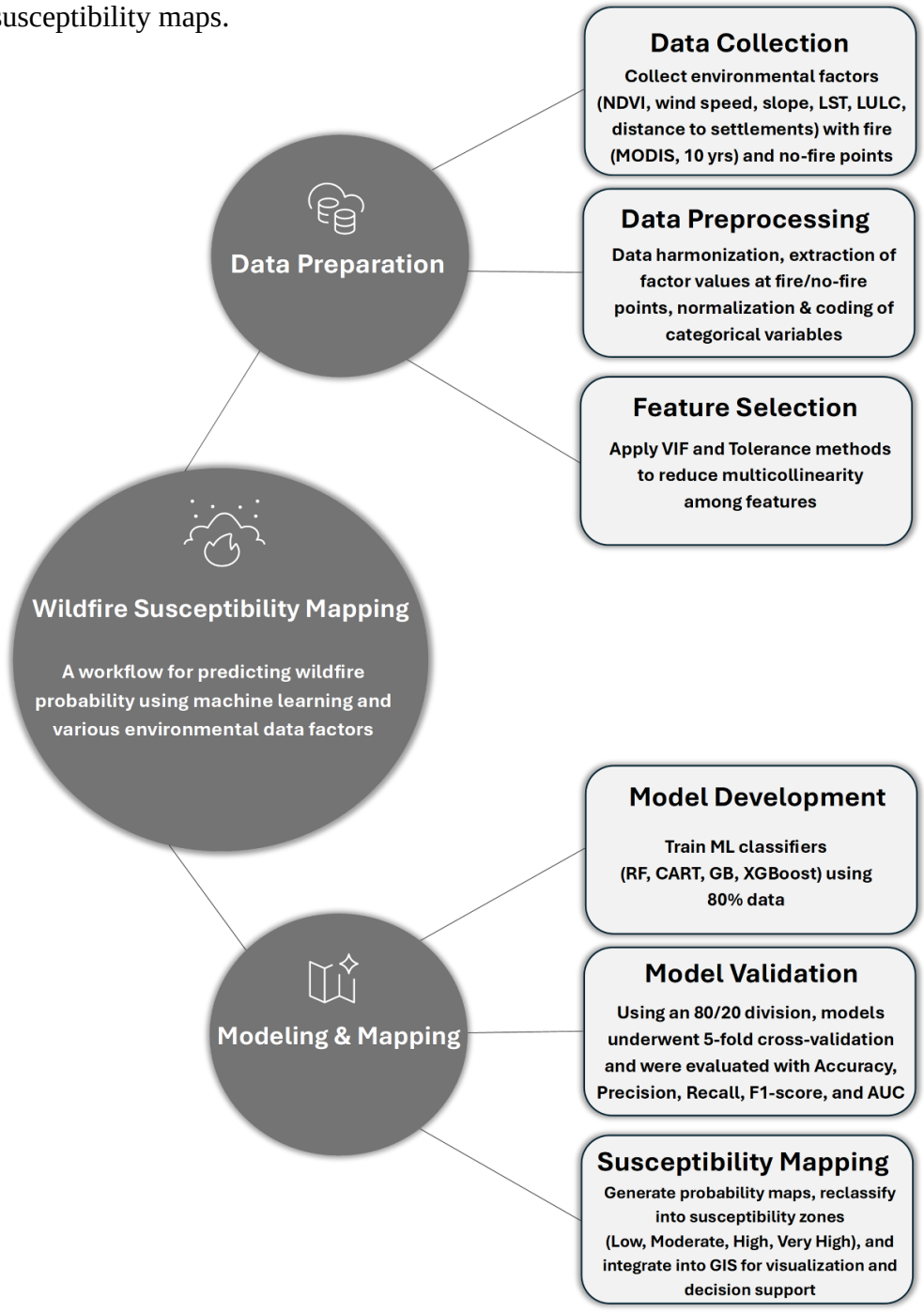

Figure 3. Workflow of wildfire susceptibility mapping in Portugal, integrating data preparation, machine learning model development, validation and mapping.

2.6 Data Preparation

The final dataset for modelling consisted of 2,000 balanced samples (1,000 fire and 1,000 no-fire) derived from the methods described in Section 2.3. The explanatory variables included vegetation (NDVI), topography (slope), land surface temperature (LST), wind speed, land cover (LULC), and distance to settlements (Section 2.4). Using a **point-based sampling approach**, values for each of these variables were extracted directly from their native-resolution raster layers at the 2,000 sample locations, ensuring that multi-resolution datasets could be consistently integrated into a single feature table for model training (Tang et al., 2022).

Before model training, the dataset was pre-processed. Categorical and continuous predictors were standardized into a compatible format, and anomalous records were removed to improve the data quality. To address the issue of multicollinearity among the explanatory variables, the **Variance Inflation Factor (VIF)** and Tolerance methods were applied (Ahmed et al., 2024). All six variables were found to have VIF values below the conventional threshold of 10, indicating no significant multicollinearity issues and confirming their suitability for inclusion in the model(El Mazi et al., 2024).

2.7 Machine Learning Models

Four distinct machine learning algorithms were employed to model wildfire susceptibility: Random Forest (RF), Classification and Regression Tree (CART), Gradient Boosting (GB), and Extreme Gradient Boosting (XGBoost).
These models were selected because of their proven performance in spatial predictions and their ability to capture both linear and nonlinear relationships among predictors.

- **Random Forest (RF):** An ensemble learning method that builds a forest of $K = 300$ decision trees $h(x, \Theta_k)$, where Θ_k represents randomness in the tree-building process. The final classification is made by aggregating all tree votes via majority voting to improve prediction stability and reduce overfitting:

  $$\hat{f}(x) = \text{mode}\{h(x, \Theta_k), k = 1, \dots, 300\}$$

  The choice of 300 trees balances model accuracy with computational efficiency(Breiman, 2001).

- **Classification and Regression Tree (CART):** CART recursively partitions the feature space into distinct regions by selecting splits that maximize the reduction in impurity, which is typically measured by the Gini index for classification:

$$Gini(t) = 1 - \sum_{i=1}^{J} p_i^2$$

where p_i is the proportion of class i observations in node t. The result is a tree of decision rules that creates homogeneous groups with respect to wildfire occurrence (Breiman et al., 2017).

- **Gradient Boosting (GB):** GB builds an additive model in a forward stage-wise manner by minimizing a differentiable loss function $L(y, F(x))$ using weak learners $h_m(x)$ added sequentially:

$$F_m(x) = F_{m-1}(x) + \nu \cdot h_m(x)$$

where ν is the learning rate, and each h_m is trained on the residuals of the previous model F_{m-1} (Friedman, 2001).

- **Extreme Gradient Boosting (XGBoost):** An optimized version of GB that includes regularization terms to control the model complexity. The objective function includes the loss function and a regularization term $\Omega(f)$:

$$\text{Obj} = \sum_i L(y_i, \hat{y}_i) + \sum_k \Omega(f_k)$$

where f_k are the decision trees, and $\Omega(f_k) = \gamma T + \frac{1}{2}\lambda \|w\|^2$ with T as the number of leaves and w the leaf weight (Chen & Guestrin, 2016).

Each model was trained on the training subset with hyperparameters optimized through a grid search, maximizing performance metrics such as accuracy, Area Under the Receiver Operating Characteristic Curve (AUC-ROC), and F1-score on a validation dataset. Cross-validation was employed to ensure the robustness of the model and mitigate overfitting.

These models complement each other by balancing bias-variance trade-offs and exploiting different strengths in handling variable interactions, missing data, and noise, making them suitable choices for spatial wildfire susceptibility prediction.

2.8 Model Validation and Feature Importance

All analyses were performed in **Python** within the Google Collab environment, using **scikit-learn** for machine learning and model evaluation, and **stats models** for multicollinearity diagnostics (Seabold & Perktold, 2010; Tonini et al., 2020).

A multi-step validation strategy was adopted to ensure the reliability of the wildfire susceptibility models. First, the explanatory variables were examined for multicollinearity using the **Variance Inflation Factor (VIF)** and **Tolerance** statistics (O'brien, 2007).

The VIF for the *i-th* predictor is defined as:

$$VIF_i = \frac{1}{1 - R_i^2}$$

where R_i^2 is the coefficient of determination of the regression of the i^{th} predictor against all other predictors. All six predictors (NDVI, slope, LST, wind speed, LULC, and distance to settlements) showed VIF values well below the threshold of 10, confirming the absence of significant multicollinearity and ensuring their suitability for the model.

For algorithmic validation, a stratified 5-fold cross-validation procedure was implemented ("Ron Kohavi," n.d.). Stratified sampling ensures that both fire and no-fire classes are proportionally represented in each fold, maintaining class balance and providing more reliable performance estimates. Each model was evaluated using four key metrics—accuracy, precision, recall, and F1-score—to comprehensively assess the overall correctness, ability to detect fire occurrences, sensitivity to actual fires, and balance between precision and recall (Sokolova & Lapalme, 2009). The performances were averaged across the folds to yield robust estimates, thereby mitigating overfitting.

Beyond cross-validation, an independent **hold-out testing** approach was employed, splitting the dataset into 80% training and 20% testing subsets (Hastie et al., 2009). The models were trained using the training subset and evaluated on the unseen testing data to confirm their predictive power and generalizability.

Feature importance was assessed using built-in scores from tree-based algorithms and the **Mean Decrease Accuracy (MDA)** method (Breiman, 2001). These complementary techniques allowed us to quantify the relative contribution of each predictor to wildfire susceptibility modeling in this study.

Finally, to validate the geostatistical interpolation of the model outputs, **a cross-validation of the Simple Kriging** method was performed in **ArcGIS Pro** (Esri, 2025). Measured values were compared against predicted values at withheld locations, and error statistics such as

Root Mean Square Error (RMSE) and **Mean Error (ME)** were calculated (Cressie, 1993a).

These metrics are defined as follows:

$$RMSE = \sqrt{\frac{1}{n}\sum_{i=1}^{n}\left(Z(s_i) - \hat{Z}(s_i)\right)^2}$$

$$ME = \frac{1}{n}\sum_{i=1}^{n}\left(Z(s_i) - \hat{Z}(s_i)\right)$$

where $Z(s_i)$ and $\hat{Z}(s_i)$ are the observed and predicted values at location s_i, $\bar{Z}$ and $\overline{\hat{Z}}$ are their respective means, and n is the number of validation points.

This additional step ensured that the interpolated susceptibility surface preserved the spatial structure of the predictions, while maintaining acceptable accuracy.

This combined validation framework—multicollinearity analysis, stratified cross-validation, hold-out testing, and feature importance diagnostics—ensured both statistical robustness and ecological interpretability of the wildfire susceptibility models.

2.9 Susceptibility Mapping

The final wildfire susceptibility map was generated by applying the best-performing machine learning model to the predictor variables across the entire study area, producing continuous wildfire probability values between 0 and 1. To account for spatial dependencies, these outputs were interpolated using the geostatistical method of **Simple Kriging** (O'Sullivan & Unwin, 2010). This method incorporates spatial autocorrelation to produce a smooth and realistic susceptibility surface compared to deterministic approaches such as Inverse Distance Weighting (IDW).

Simple Kriging estimates the value at an unsampled location s_0 as a weighted sum of observed values:

$$\hat{Z}(s_0) = \sum_{i=1}^{n} \lambda_i Z(s_i)$$

where $Z(s_i)$ are the known values at locations s_i, and weights λ_i are calculated based on the spatial covariance structure between the points to minimize estimation variance and ensure unbiasedness(Cressie, 1993).

The interpolated susceptibility surface was reclassified into four risk levels: very low (0.00–0.25), moderate (0.25–0.50), high (0.50–0.75), and very high (0.75–1.00) (Losasso et al., 2017). These thresholds were defined based on exploratory data analysis and expert consultation to support meaningful interpretation for fire risk management.

The uncertainty of the Kriging interpolation was examined through cross-validation in **ArcGIS Pro (Geostatistical Wizard)**, where predicted values were compared with observed samples. The full validation metrics are presented in the Results section.

The integration of machine learning predictions with geostatistical interpolation produced a wildfire susceptibility map that is both statistically robust and spatially coherent, offering valuable insights to guide targeted fire prevention and mitigation strategies.

3. Results

3.1 Variable Analysis and Multicollinearity

Before developing the wildfire susceptibility model, it was essential to evaluate the predictor variables to ensure their relevance to wildfire occurrence and to confirm statistical independence. Multicollinearity among explanatory variables can distort model estimates and reduce predictive reliability, especially in machine learning techniques such as Random Forest (Breiman, 2001; Dormann et al., 2013). To address this, six environmental and anthropogenic variables were examined—Land Use/Land Cover (LULC), Normalized Difference Vegetation Index (NDVI), Land Surface Temperature (LST), Slope, Wind Speed, and Distance to Settlements—and their spatial distribution was analysed alongside a statistical multicollinearity assessment using Variance Inflation Factor (VIF) and tolerance values.

The spatial distributions of these predictor variables are illustrated in Figure 4, with each subfigure highlighting a specific environmental factor. Land use and land cover (a) reflect the spatial extent of forests, agriculture, bare soil, and built-up areas, where forest-dominated zones, particularly in mountainous regions, correspond to areas of high fuel accumulation, and thus increased wildfire susceptibility (Vanderhoof & Hawbaker, 2018).
The Normalized Difference Vegetation Index (b) measures vegetation density, where high NDVI values indicate dense vegetation that serves as potential fuel for aiding fire ignition and spread. Land Surface Temperature (c) captures thermal variation, with elevated temperatures in exposed lowlands and urban regions coinciding with higher ignition probabilities (Vermote et al., 2016). Terrain slope (d) affects fire behaviour by accelerating upslope spread, as steeper areas promote the preheating of vegetation (Woodall & Nagel, 2007). Wind speed (e) influences fire dynamics, increasing spread rates, and determining direction, with higher wind speeds correlating with elevated wildfire hazards (Stephens, 2001).
Finally, the distance to settlements (f) reflects anthropogenic ignition pressure, with areas closer to urban clusters exhibiting elevated ignition potential (Grala, R. K. & D'Agata, P. J., 2024).

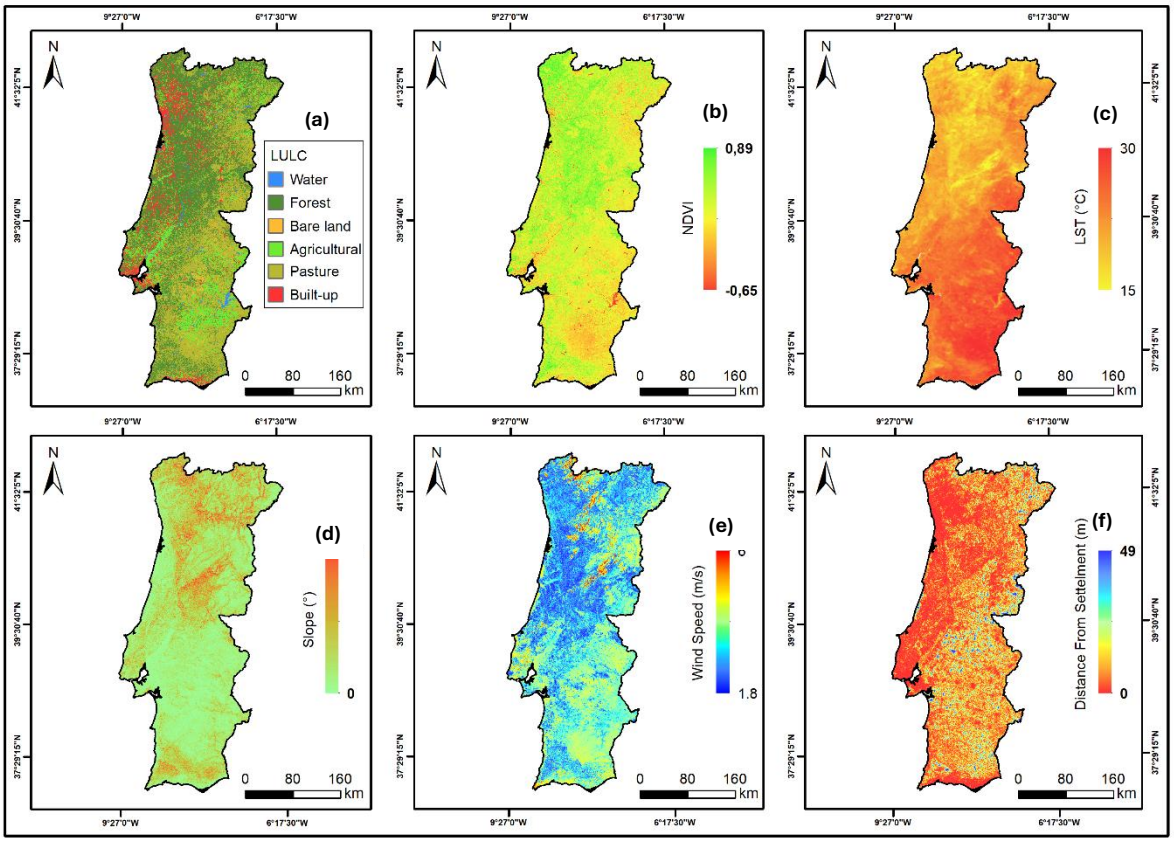

Figure 4. Spatial distribution of wildfire predictor variables: (a) LULC, (b) NDVI, (c) LST, (d) Slope, (e) Wind Speed, and (f) Distance to Settlements.

Multicollinearity was further assessed through VIF and tolerance metrics for each predictor (Figure 5). These statistics demonstrate the degree of correlation between each variable and the others. All six predictors exhibited VIF values between 2.5 and 3.9, well within acceptable limits (threshold < 10), and tolerance values ranging from 0.26 to 0.69, exceeding the common cut-off of 0.1 (O'brien, 2007).

For instance, NDVI (VIF = 2.6; tolerance = 0.39) and LST (VIF = 3.3; tolerance = 0.30) showed a moderate correlation, as expected owing to biophysical links, but remained statistically independent. Similarly, Wind Speed (VIF = 3.4; tolerance = 0.29) and Distance to Settlements (VIF = 3.9; tolerance = 0.26) did not exhibit problematic collinearity.

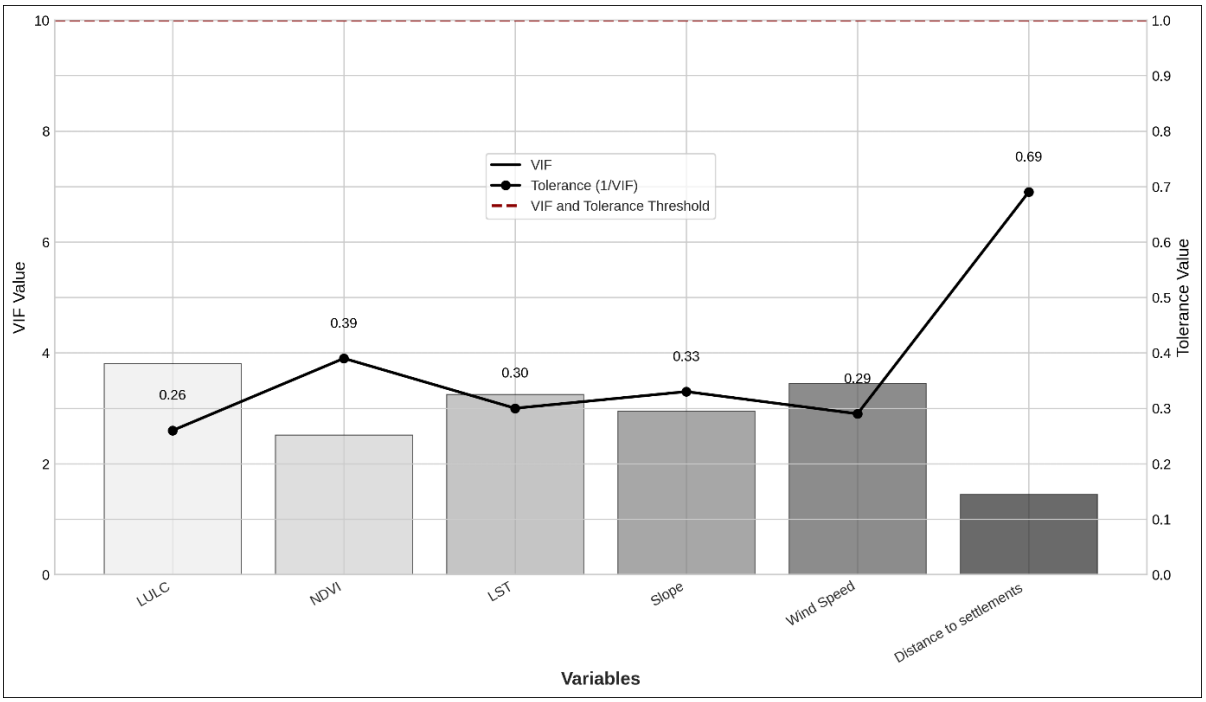

Figure 5. Variance Inflation Factor (VIF) and Tolerance values for wildfire predictor variables.

The combined spatial and statistical analyses confirmed that the selected variables were ecologically meaningful and statistically independent.
This supports their integration within the Random Forest modeling framework, ensuring the stability and reliability of wildfire susceptibility predictions. Hence, the six variables— land use/land cover (LULC), NDVI, LST, slope, wind speed, and distance to settlements — were retained for subsequent modeling stages.

3.2 Model Performance and Cross-Validation

After validating the selected variables, the next step was to evaluate the performance of the machine learning models used in this study. To provide a clear comparison, Table 2 summarizes the key performance metrics obtained for each model—Random Forest (RF), Classification and Regression Trees (CART), Gradient Boosting (GB), and Extreme Gradient Boosting (XGB)—based on 5-fold stratified cross-validation (Chen & Guestrin, 2016).

Table 2 presents the average values of Accuracy, Precision, Recall, and F1-Score for all models.

Model	Accuracy	Precision	Recall	F1-Score
Random Forest	0.9293	0.9315	0.9313	0.9309
CART	0.8927	0.9012	0.8886	0.8939
Gradient Boosting	0.9272	0.9307	0.9271	0.9287
XGBoost	0.9298	0.9311	0.9323	0.9315

These metrics provide a comprehensive understanding of each model's ability to correctly classify instances while accounting for both false positives and false negatives (Sokolova & Lapalme, 2009).

As shown in the table, XGBoost (Chen & Guestrin, 2016) achieved the highest overall performance, with an accuracy of 92.98%, precision of 93.11%, recall of 93.23%, and an F1-score of 93.15%. It was closely followed by Random Forest (Breiman, 2001) and Gradient Boosting, with CART lagging slightly behind in all metrics.

Figure 6 provides a visual comparison of these scores using bar charts, facilitating a quick assessment of the relative model performance.

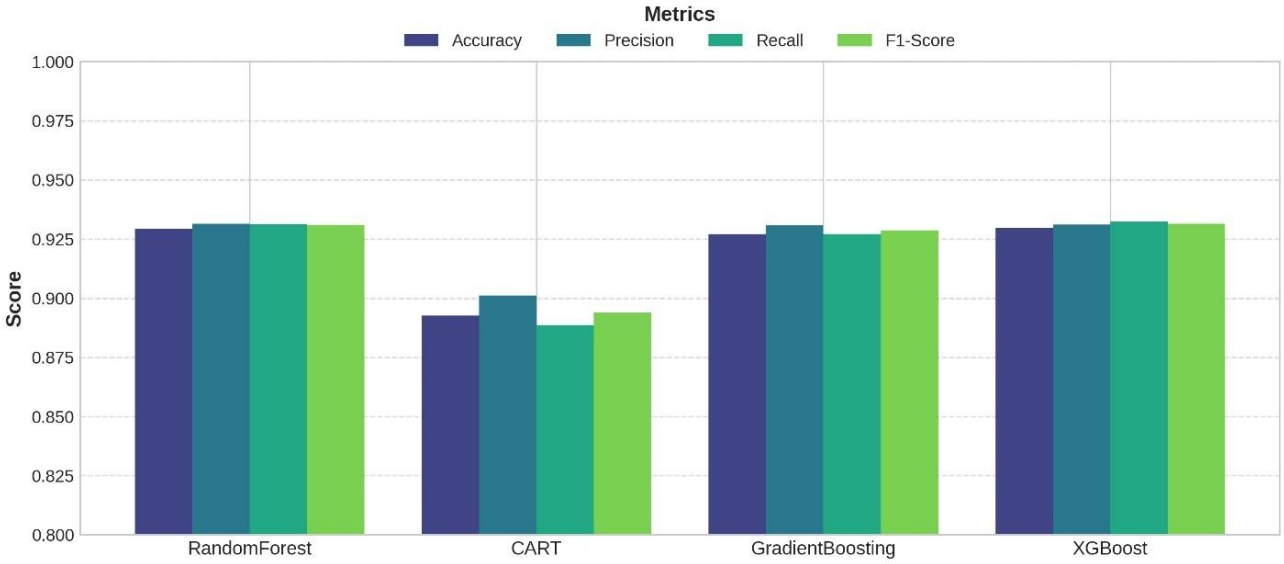

	Accuracy	Precision	Recall	F1-Score
RandomForest	0.9293	0.9315	0.9313	0.9309
CART	0.8927	0.9012	0.8886	0.8939
GradientBoosting	0.9272	0.9307	0.9271	0.9287
XGBoost	0.9298	0.9311	0.9323	0.9315

Figure 6. Comparison of Model Performance Metrics (Accuracy, Precision, Recall, F1-Score) across RF, CART, GB, and XGB models.

To further assess the classification quality, Figure 7 displays the ROC curves for all models along with their Area Under the Curve (AUC) values (Fawcett, 2006). The ROC curve analysis corroborated the quantitative metrics, showing that XGBoost and Random Forest exhibited near-identical and superior AUC scores (0.98), indicating excellent discriminatory ability. CART, with an AUC of 0.88, performed notably worse in comparison.

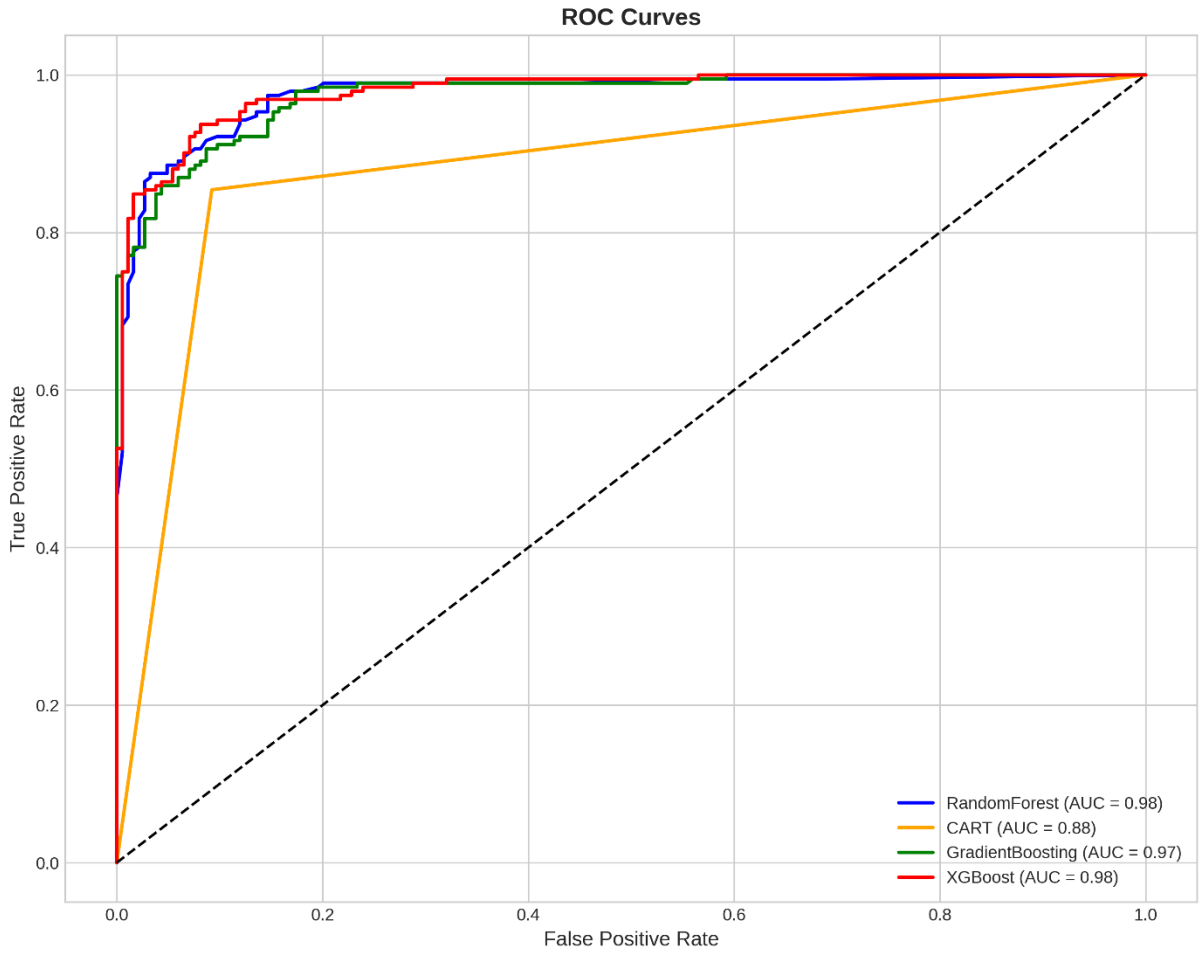

Figure 7. ROC Curves and AUC values of the RF, CART, GB, and XGB models.

Overall, based on the cross-validation results and ROC analysis, XGBoost was identified as the best-performing model. Its slightly higher metrics and strong ROC performance justify its selection for subsequent analysis and final prediction.

3.3 Wildfire Susceptibility Maps and Area Statistics

The spatial distribution of wildfire susceptibility across the study area was modelled using four machine learning approaches: Random Forest (RF) (Breiman, 2001), Classification and Regression Trees (CART) (Breiman et al., 2017), Gradient Boosting (GB) (Friedman, 2001), and Extreme Gradient Boosting (XGB) (Chen & Guestrin, 2016). The resulting susceptibility maps (Figure 8) classified the territory into four fire risk categories: Low, Medium, High, and Very High.

The visual examination of the wildfire susceptibility maps (Figure 8) revealed a coherent spatial distribution across all four machine learning models. Predominantly, the central and northern regions exhibit extensive areas classified as having high and very high susceptibility, corresponding closely to forested and mountainous terrains known for elevated fuel loads and complex topography (Catry et al., 2010). Importantly, isolated pockets of very high susceptibility were also evident in the southern part of the study area, underscoring localized conditions that may facilitate fire ignition and spread despite generally sparser vegetation. While the broad spatial patterns remained consistent, subtle differences in the extent and delineation of high-risk zones were apparent among the models, reflecting inherent variations in the handling of predictor interactions and algorithmic sensitivity.

To quantitatively assess these variations, the classified maps were overlaid with the national boundary, and the areal extent of each susceptibility class was calculated (Table 3), as follows: Across models, approximately 30–32% of the study area fell under the low susceptibility category, while 18–20% was classified as Very High susceptibility. The proportion of high-susceptibility zones ranged between 23% and 28%, with Gradient Boosting identifying the largest share (27.62%) of high-risk areas. Random Forest and CART yielded relatively balanced distributions across classes, whereas XGBoost allocated a slightly higher proportion to the Very High class (19.41%), consistent with its superior performance demonstrated in the cross-validation analysis.

The probabilistic model outputs were interpolated into continuous susceptibility surfaces using the Simple Kriging method (Diggle et al., 2003). Cross-validation of the kriging interpolation resulted in moderate accuracy, with a Root Mean Square Error (RMSE) of 0.1462 (normalized between 0 and 1) (Chai & Draxler, 2014), indicating that average prediction errors account for approximately 15% of the data range. The Mean Error (ME) was very close to zero (+0.00044), confirming the unbiased nature of the interpolated predictions. This suggests that while the interpolation effectively captures broad spatial trends, finer local variations may be less accurately represented.

Together, the wildfire susceptibility maps and area statistics highlight the pronounced spatial heterogeneity of fire risk in the region. Although all models broadly agree on the identification of northern and central hotspots, differences in class area proportions provide valuable insights into prioritizing fire prevention and management strategies. Among the tested algorithms, XGBoost emerged as the most robust, combining high predictive accuracy with realistic spatial delineation of elevated fire-risk zones.

Table 3. Area distribution of wildfire susceptibility classes (Low, Medium, High, Very High) across RF, CART, GB, and XGB models.

Models	Distribution	Susceptibility classes			
		Low	Medium	High	Very High
Random Forest	Area (km²)	29,791.47	17,353.24	24,919.67	17,726.19
	Percentage (%)	30.68	17.85	25.65	18.82
CART	Area (km²)	29,791.47	19,356.30	22,105.26	17,438.45
	Percentage (%)	31.70	20.59	23.52	18.55
Gradient Boosting	Area (km²)	28,531.84	17,663.21	25,519.84	16,976.59
	Percentage (%)	30.87	19.11	27.62	18.38
Extreme Gradient Boosting	Area (km²)	29,524.72	17,848.45	22,910.43	18,407.88
	Percentage (%)	31.12	18.81	24.16	19.41

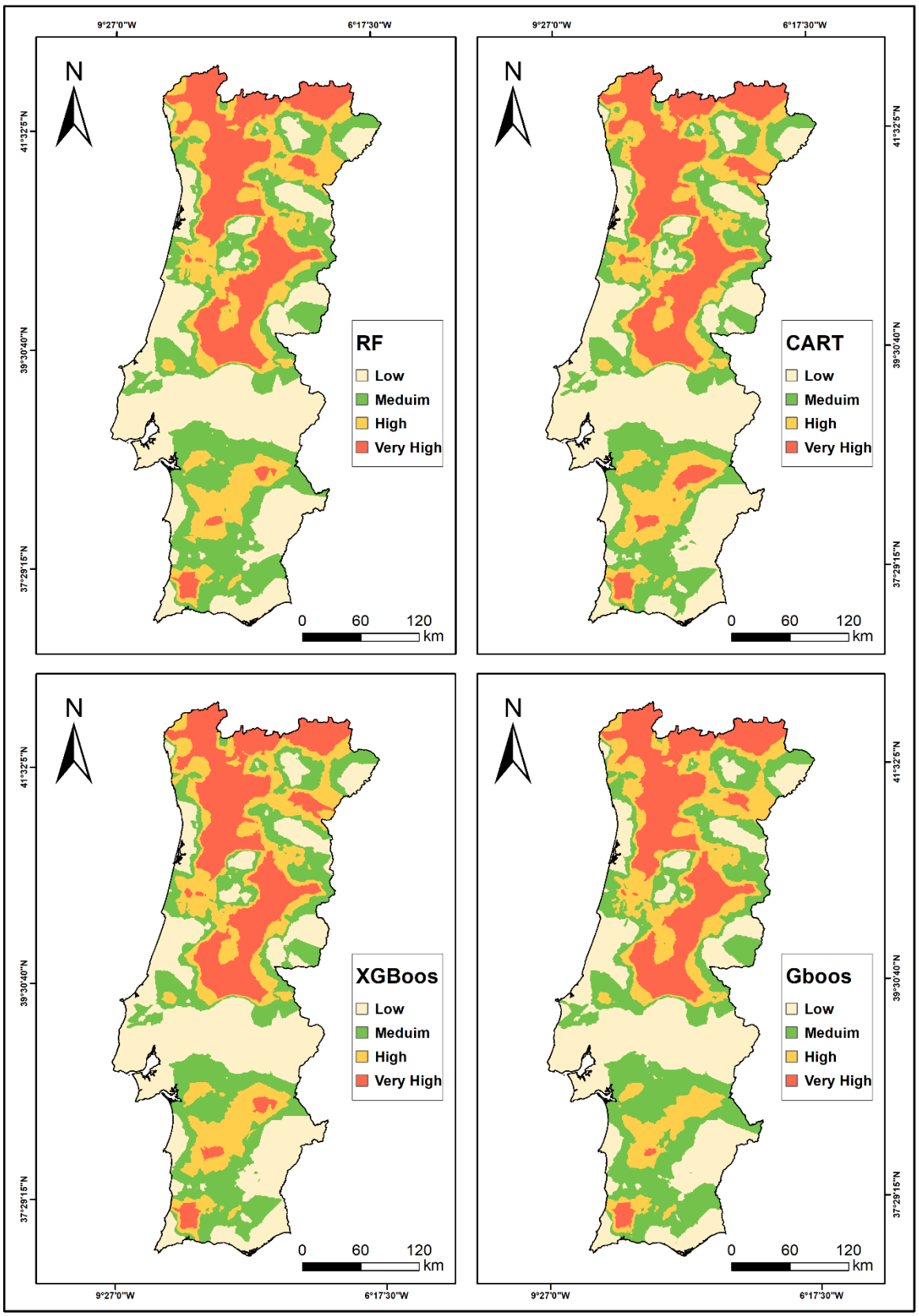

Figure 8. Wildfire susceptibility maps derived from RF, CART, GB, and XGB models.

3.4 Feature Importance and MDA

To better understand the contribution of each explanatory factor in shaping wildfire susceptibility, a feature importance analysis was performed using both built-in model importance scores and Mean Decrease Accuracy (MDA), obtained through permutation analysis (Altmann et al., 2010). These complementary approaches quantify the strength of influence of each variable on the predictions, thereby providing insights into the ecological and environmental drivers of wildfire risk.

Figure 9. Relative Feature Importance and Mean Decrease Accuracy (MDA) Scores for Wildfire Predictors.

The heatmap in Figure 9 summarizes the relative importance of the six predictor variables across the four classifiers (Random Forest, CART, Gradient Boosting, and XGBoost). Two consistent patterns were observed.

- **NDVI** (vegetation greenness) was the most influential variable across nearly all models and both metrics, highlighting the central role of vegetation density and fuel availability in the occurrence of wildfires (Chuvieco et al., 2008).
- **Slope** and **LULC** were ranked as secondary but important predictors, indicating that topography and land cover structure also strongly modulate susceptibility patterns.
- **LST** and **wind speed** contributed moderately, reflecting their role as climatic and micro-environmental conditions influencing ignition and spread.
- **Distance to settlements** generally showed the lowest influence, though still non-negligible, suggesting that anthropogenic proximity is a factor but is less dominant than biophysical conditions.

The use of both feature importance and MDA strengthens the robustness of the findings: while raw importance highlights model-specific contributions, MDA provides a measure of predictive loss when each variable is permuted (Tonini et al., 2020). Together, these analyses confirmed that vegetation condition (NDVI), terrain (slope), and land cover type (LULC) are the most decisive factors driving wildfire susceptibility in the study area.
This provides valuable ecological insights into both the spatial drivers of fire risk and the interpretability of machine learning predictions.

4. Discussion

The findings of this study offer significant insights into the spatial patterns and primary determinants of wildfire susceptibility in Portugal.
In contrast to numerous prior studies that predominantly utilized a single machine learning classifier, this study systematically compared four algorithms— random forest, CART, gradient boosting, and XGBoost—employing six explanatory variables to produce robust susceptibility maps. This comparative framework enhances model reliability and contributes to the expanding body of literature that assesses the strengths and limitations of ensemble learning approaches for wildfire prediction (Bhowmik et al., 2023; Bjånes et al., 2021).

The analysis of variable importance indicated that vegetation-related factors, particularly NDVI and LULC, were the most influential predictors of wildfire susceptibility in the study area. These findings align with ecological studies that highlight the role of fuel availability and type in influencing ignition likelihood and fire spread (Chávez et al., 2011; Fernandes & Botelho, 2003).
Topographic variables such as slope and climatic variables, including wind speed, also proved significant, corroborating their well-established influence on fire behaviour (Parisien et al., 2016).
The relatively lower weight of anthropogenic variables, such as distance to settlements, suggests that biophysical conditions remain the dominant drivers of susceptibility in Portugal.
Model performance evaluation confirmed the superior predictive capability of the ensemble techniques, with XGBoost achieving the highest accuracy (92.98%) and AUC (0.98). These values are comparable to, and in some cases exceed, those reported in recent wildfire susceptibility studies across Mediterranean and other fire-prone landscapes (Chuvieco et al, 2019; Rodrigues et al, 2021). The high predictive skill demonstrates the ability of XGBoost to capture complex, nonlinear relationships between environmental conditions and fire occurrence.

The final susceptibility maps consistently identified the northern and central interior regions as the most fire-prone, in line with historical fire records and prior research on Portuguese fire regimes (Calheiros et al., 2022; European Commission. Joint Research Centre., 2023).
Quantitative area statistics further underscored the dominance of the "Very High" susceptibility category in these zones. These outputs not only validate the modelling framework but also offer actionable insights into fire management, land-use planning, and resource prioritization.

Nevertheless, certain limitations must be acknowledged. The spatial resolution of certain variables, such as LST and wind speed, may not capture micro-scale heterogeneity, whereas the fire occurrence dataset may be subject to sampling bias and underreporting. These factors, which are often not stable and can change over time, could influence the model's predictive precision at local scales. Future research should integrate higher-resolution environmental datasets, adopt multi-temporal variables to account for seasonal variability, and test hybrid

approaches combining remote sensing with socio-economic drivers to build a more comprehensive and robust model.

5. Conclusion

This study demonstrated the efficacy of machine learning, with a particular focus on XGBoost, in mapping wildfire susceptibility in Portugal.

Through a systematic comparison of four classifiers and six explanatory variables, this study confirmed that vegetation (NDVI, LULC) and topography (slope) are the primary determinants of fire occurrence. The resulting susceptibility maps identified northern and central Portugal as the regions most prone to fires, closely aligning with historical fire records. Despite certain limitations related to variable resolution and potential sampling bias, the framework provides reliable and transferable tools for supporting fire management, land-use planning, and risk reduction. Future research should incorporate finer-scale environmental and socioeconomic data to further enhance predictive performance.

References:

Ahmed, R. R., Streimikiene, D., Streimikis, J., & Siksnelyte-Butkiene, I. (2024). A comparative analysis of multivariate approaches for data analysis in management sciences. *E+M Ekonomie a Management*, *27*(1), 192–210. https://doi.org/10.15240/tul/001/2024-5-001

Almeida, P., Menezes, I. C., & Miranda, A. I. (2024). A Human Behavior Wildfire Ignition Probability Index for Application to Mainland Portugal. *Fire*, *7*(12), 447. https://doi.org/10.3390/fire7120447

Altmann, A., Toloşi, L., Sander, O., & Lengauer, T. (2010). Permutation importance: A corrected feature importance measure. *Bioinformatics*, *26*(10), 1340–1347. https://doi.org/10.1093/bioinformatics/btq134

Bhowmik, R. T., Jung, Y. S., Aguilera, J. A., Prunicki, M., & Nadeau, K. (2023). A multi-modal wildfire prediction and early-warning system based on a novel machine learning framework. *Journal of Environmental Management*, *341*, 117908. https://doi.org/10.1016/j.jenvman.2023.117908

Bjånes, A., De La Fuente, R., & Mena, P. (2021). A deep learning ensemble model for wildfire susceptibility mapping. *Ecological Informatics*, *65*, 101397. https://doi.org/10.1016/j.ecoinf.2021.101397

Breiman, L. (2001). Random Forests. *Machine Learning*, *45*(1), 5–32. https://doi.org/10.1023/A:1010933404324

Breiman, L., Friedman, J. H., Olshen, R. A., & Stone, C. J. (2017). *Classification And Regression Trees* (1st ed.). Routledge. https://doi.org/10.1201/9781315139470

Brown, C. F., Brumby, S. P., Guzder-Williams, B., Birch, T., Hyde, S. B., Mazzariello, J., Czerwinski, W., Pasquarella, V. J., Haertel, R., Ilyushchenko, S., Schwehr, K., Weisse, M., Stolle, F., Hanson, C., Guinan, O., Moore, R., & Tait, A. M. (2022). Dynamic World, Near real-time global 10 m land use land cover mapping. *Scientific Data*, *9*(1), 251. https://doi.org/10.1038/s41597-022-01307-4

Calheiros, T., Benali, A., Pereira, M., Silva, J., & Nunes, J. (2022). Drivers of extreme burnt area in Portugal: Fire weather and vegetation. *Natural Hazards and Earth System Sciences*, *22*(12), 4019–4037. https://doi.org/10.5194/nhess-22-4019-2022

Catry, F. X., Rego, F., Moreira, F., Fernandes, P. M., & Pausas, J. G. (2010). Post-fire tree mortality in mixed forests of central Portugal. *Forest Ecology and Management*, *260*(7), 1184–1192. https://doi.org/10.1016/j.foreco.2010.07.010

Central Intelligence Agency. (2025). *The World Factbook: Portugal*. The World Factbook. https://www.cia.gov/the-world-factbook/countries/portugal/

Chai, T., & Draxler, R. R. (2014). Root mean square error (RMSE) or mean absolute error (MAE)? – Arguments against avoiding RMSE in the literature. *Geoscientific Model Development*, *7*(3), 1247–1250. https://doi.org/10.5194/gmd-7-1247-2014

Chávez, C. A., Stranlund, J. K., & Gómez, W. (2011). Controlling urban air pollution caused by households: Uncertainty, prices, and income. *Journal of Environmental Management*, *92*(10), 2746–2753. https://doi.org/10.1016/j.jenvman.2011.06.014

Chen, T., & Guestrin, C. (2016). XGBoost: A Scalable Tree Boosting System. *Proceedings of the 22nd ACM SIGKDD International Conference on Knowledge Discovery and Data Mining*, 785–794. https://doi.org/10.1145/2939672.2939785

Chuvieco, E., Giglio, L., & Justice, C. (2008). Global characterization of fire activity: Toward defining fire regimes from Earth observation data. *Global Change Biology*, *14*(7), 1488–1502. https://doi.org/10.1111/j.1365-2486.2008.01585.x

Chuvieco, E., Mouillot, F., Van Der Werf, G. R., San Miguel, J., Tanase, M., Koutsias, N., García, M., Yebra, M., Padilla, M., Gitas, I., Heil, A., Hawbaker, T. J., & Giglio, L. (2019). Historical background and current developments for mapping burned area from satellite Earth observation. *Remote Sensing of Environment*, *225*, 45–64. https://doi.org/10.1016/j.rse.2019.02.013

Cressie, N. A. C. (1993). *Statistics for Spatial Data* (1st ed.). Wiley. https://doi.org/10.1002/9781119115151

Diggle, P. J., Ribeiro, P. J., & Christensen, O. F. (2003). An Introduction to Model-Based Geostatistics. In J. Møller (Ed.), *Spatial Statistics and Computational Methods* (Vol. 173, pp. 43–86). Springer New York. https://doi.org/10.1007/978-0-387-21811-3_2

Dormann, C. F., Elith, J., Bacher, S., Buchmann, C., Carl, G., Carré, G., Marquéz, J. R. G., Gruber, B., Lafourcade, B., Leitão, P. J., Münkemüller, T., McClean, C., Osborne, P. E., Reineking, B., Schröder, B., Skidmore, A. K., Zurell, D., & Lautenbach, S. (2013). Collinearity: A review of methods to deal with it and a simulation study evaluating their performance. *Ecography*, *36*(1), 27–46. https://doi.org/10.1111/j.1600-0587.2012.07348.x

El Mazi, M., Boutallaka, M., Saber, E., Chanyour, Y., & Bouhlal, A. (2024). Forest fire risk modeling in Mediterranean forests using GIS and AHP method: Case of the high Rif forest massif (Morocco). *Euro-Mediterranean Journal for Environmental Integration*, *9*(3), 1109–1123. https://doi.org/10.1007/s41207-024-00591-3

Esri. (2025). *ArcGIS Pro (Geostatistical Analyst extension)* (Version 3.3) [Computer software]. https://www.esri.com/en-us/arcgis/products/arcgis-pro/overview

European Commission, J. R. C. (2025). *Current wildfire situation in Europe*. https://joint-research-centre.ec.europa.eu/projects-and-activities/natural-and-man-made-hazards/fires/current-wildfire-situation-europe

European Commission. Joint Research Centre. (2023). *Advance report on forest fires in Europe, Middle East and North Africa 2022.* Publications Office. https://data.europa.eu/doi/10.2760/091540

European Commission. Joint Research Centre. (2024). *GHSL country Statistics by degree of urbanization: Public release of GHS COUNTRY STATS R2024A.* Publications Office. https://data.europa.eu/doi/10.2760/0075418

Eurostat. (2025). *Land cover statistics for Portugal*. Eurostat. https://ec.europa.eu/eurostat/statistics-explained/index.php/Land_cover_statistics

Farr, T. G., Rosen, P. A., Caro, E., Crippen, R., Duren, R., Hensley, S., Kobrick, M., Paller, M., Rodriguez, E., Roth, L., Seal, D., Shaffer, S., Shimada, J., Umland, J., Werner, M., Oskin, M., Burbank, D., & Alsdorf, D. (2007). The Shuttle Radar Topography Mission. *Reviews of Geophysics*, *45*(2), 2005RG000183. https://doi.org/10.1029/2005RG000183

Fawcett, T. (2006). An introduction to ROC analysis. *Pattern Recognition Letters*, *27*(8), 861–874. https://doi.org/10.1016/j.patrec.2005.10.010

Fernandes, P. M., & Botelho, H. S. (2003). A review of prescribed burning effectiveness in fire hazard reduction. *International Journal of Wildland Fire*, *12*(2), 117. https://doi.org/10.1071/WF02042

Friedman, J. H. (2001). Greedy function approximation: A gradient boosting machine. *The Annals of Statistics*, *29*(5). https://doi.org/10.1214/aos/1013203451

Giglio, L., Schroeder, W., & Justice, C. O. (2016). The collection 6 MODIS active fire detection algorithm and fire products. *Remote Sensing of Environment*, *178*, 31–41. https://doi.org/10.1016/j.rse.2016.02.054

Grala, R. K. & D'Agata, P. J. (2024). Assessing human-caused wildfire risk using GIS Authors. *Fire Management Today*.

Hastie, T., Tibshirani, R., & Friedman, J. (2009). *The Elements of Statistical Learning*. Springer New York. https://doi.org/10.1007/978-0-387-84858-7

ICNF (Instituto da Conservação da Natureza e das Florestas). (2025). *Estatísticas dos Incêndios Rurais (Rural Fire Statistics)*. Instituto da Conservação da Natureza e das Florestas. https://icnf.pt/

Jaafari, A., & Pourghasemi, H. R. (2019). Factors Influencing Regional-Scale Wildfire Probability in Iran. In *Spatial Modeling in GIS and R for Earth and Environmental Sciences* (pp. 607–619). Elsevier. https://linkinghub.elsevier.com/retrieve/pii/B9780128152263000284

Losasso, L., Rinaldi, C., Alberico, D., & Sdao, F. (2017). Landslide Risk Analysis Along Strategic Touristic Roads in Basilicata (Southern Italy) Using the Modified RHRS 2.0 Method. In O. Gervasi, B. Murgante, S. Misra, G. Borruso, C. M. Torre, A. M. A. C. Rocha, D. Taniar, B. O. Apduhan, E. Stankova, & A. Cuzzocrea (Eds.), *Computational Science and Its Applications – ICCSA 2017* (Vol. 10404, pp. 761–776). Springer International Publishing. https://doi.org/10.1007/978-3-319-62392-4_55

Muñoz-Sabater, J., Dutra, E., Agustí-Panareda, A., Albergel, C., Arduini, G., Balsamo, G., Boussetta, S., Choulga, M., Harrigan, S., Hersbach, H., Martens, B., Miralles, D. G., Piles, M., Rodríguez-Fernández, N. J., Zsoter, E., Buontempo, C., & Thépaut, J.-N. (2021). ERA5-Land: A state-of-the-art global reanalysis dataset for land applications. *Earth System Science Data*, *13*(9), 4349–4383. https://doi.org/10.5194/essd-13-4349-2021

O'brien, R. M. (2007). A Caution Regarding Rules of Thumb for Variance Inflation Factors. *Quality & Quantity*, *41*(5), 673–690. https://doi.org/10.1007/s11135-006-9018-6

Oliveira, S., & Zêzere, J. L. (2020). Assessing the biophysical and social drivers of burned area distribution at the local scale. *Journal of Environmental Management*, *264*, 110449. https://doi.org/10.1016/j.jenvman.2020.110449

O'Sullivan, D., & Unwin, D. J. (2010). *Geographic Information Analysis* (1st ed.). Wiley. https://doi.org/10.1002/9780470549094

Parente, J., Pereira, M. G., Amraoui, M., & Fischer, E. M. (2018). Heat waves in Portugal: Current regime, changes in future climate and impacts on extreme wildfires. *Science of The Total Environment*, *631–632*, 534–549. https://doi.org/10.1016/j.scitotenv.2018.03.044

Parisien, M.-A., Miller, C., Parks, S. A., DeLancey, E. R., Robinne, F.-N., & Flannigan, M. D. (2016). The spatially varying influence of humans on fire probability in North America. *Environmental Research Letters*, *11*(7), 075005. https://doi.org/10.1088/1748-9326/11/7/075005

Rodrigues, M., Mariani, M., Russo, A., Salis, M., Galizia, L. F., & Cardil, A. (2021). Spatio-Temporal Domains of Wildfire-Prone Teleconnection Patterns in the Western Mediterranean Basin. *Geophysical Research Letters*, *48*(19), e2021GL094238. https://doi.org/10.1029/2021GL094238

Ron Kohavi. (n.d.). *1995*, 7.

Sabater, S., Elosegi, A., & Ludwig, R. (2021). Framing biophysical and societal implications of multiple stressor effects on river networks. *Science of The Total Environment*, *753*, 141973. https://doi.org/10.1016/j.scitotenv.2020.141973

Seabold, S., & Perktold, J. (2010). *Statsmodels: Econometric and Statistical Modeling with Python*. 92–96. https://doi.org/10.25080/Majora-92bf1922-011

Sokolova, M., & Lapalme, G. (2009). A systematic analysis of performance measures for classification tasks. *Information Processing & Management*, *45*(4), 427–437. https://doi.org/10.1016/j.ipm.2009.03.002

Stephens, S. L. (2001). Fire history differences in adjacent Jeffrey pine and upper montane forests in the eastern Sierra Nevada. *International Journal of Wildland Fire*, *10*(2), 161. https://doi.org/10.1071/WF01008

Tang, X., Machimura, T., Li, J., Yu, H., & Liu, W. (2022). Evaluating Seasonal Wildfire Susceptibility and Wildfire Threats to Local Ecosystems in the Largest Forested Area of China. *Earth's Future*, *10*(5), e2021EF002199. https://doi.org/10.1029/2021EF002199

Tonini, M., D'Andrea, M., Biondi, G., Degli Esposti, S., Trucchia, A., & Fiorucci, P. (2020). A Machine Learning-Based Approach for Wildfire Susceptibility Mapping. The Case Study of the Liguria Region in Italy. *Geosciences*, *10*(3), 105. https://doi.org/10.3390/geosciences10030105

Turco, M., Jerez, S., Augusto, S., Tarín-Carrasco, P., Ratola, N., Jiménez-Guerrero, P., & Trigo, R. M. (2019). Climate drivers of the 2017 devastating fires in Portugal. *Scientific Reports*, *9*(1), 13886. https://doi.org/10.1038/s41598-019-50281-2

Turco, M., Von Hardenberg, J., AghaKouchak, A., Llasat, M. C., Provenzale, A., & Trigo, R. M. (2017). On the key role of droughts in the dynamics of summer fires in Mediterranean Europe. *Scientific Reports*, *7*(1), 81. https://doi.org/10.1038/s41598-017-00116-9

Vanderhoof, M. K., & Hawbaker, T. J. (2018). It matters when you measure it: Using snow-cover Normalised Difference Vegetation Index (NDVI) to isolate post-fire conifer regeneration. *International Journal of Wildland Fire*, *27*(12), 815. https://doi.org/10.1071/WF18075

Verde, J. C., & Zêzere, J. L. (2010). Assessment and validation of wildfire susceptibility and hazard in Portugal. *Natural Hazards and Earth System Sciences*, *10*(3), 485–497. https://doi.org/10.5194/nhess-10-485-2010

Vermote, E., Justice, C., Claverie, M., & Franch, B. (2016). Preliminary analysis of the performance of the Landsat 8/OLI land surface reflectance product. *Remote Sensing of Environment*, *185*, 46–56. https://doi.org/10.1016/j.rse.2016.04.008

Wan, Z., Hook, S., & Hulley, G. (2021). *MODIS/Terra Land Surface Temperature/Emissivity 8-Day L3 Global 1km SIN Grid V061* [Dataset]. NASA Land Processes Distributed Active Archive Center. https://doi.org/10.5067/MODIS/MOD11A2.061

Woodall, C. W., & Nagel, L. M. (2007). Downed woody fuel loading dynamics of a large-scale blowdown in northern Minnesota, U.S.A. *Forest Ecology and Management*, *247*(1–3), 194–199. https://doi.org/10.1016/j.foreco.2007.04.040